

## NOTE

# Numerical Treatment of Polar Coordinate Singularities

Kamran Mohseni and Tim Colonius

*Division of Engineering and Applied Science, 104-44, California Institute of Technology,  
Pasadena, California 91125*

E-mail: mohseni@caltech.edu, colonius@caltech.edu

Received May 21, 1999; revised September 20, 1999

### 1. INTRODUCTION

The treatment of the geometrical singularity in cylindrical and spherical coordinates has for many years been a difficulty in the development of accurate finite difference (FD) and pseudo-spectral (PS) schemes. A variety of numerical procedures for dealing with the singularity have been suggested. For comparative purposes, some of these are discussed in the next sections, but the reader is referred to several books and review papers [3, 7, 10] for more detailed references.

Generally, methods discussed in the literature use pole equations, which are akin to boundary conditions to be applied at the singular point. The treatment of the pole as a computational boundary can lead to numerical difficulties. These include the necessity of special boundary closures for FD schemes (e.g., [11]), undesirable clustering of grid points in PS schemes (e.g., [12]), and, in FD schemes, the generation of spurious waves which oscillate from grid point to grid point (so-called two-delta or sawtooth waves, see [4, 26]).

In the present paper we investigate a method for treating the coordinate singularity whereby singular coordinates are redefined so that data are differentiated smoothly through the pole, and we avoid placing a grid point directly at the pole. This eliminates the need for any pole equation. Despite the simplicity of the present technique, it appears to be an effective and systematic way to treat many scalar and vector equations in cylindrical and spherical coordinates. A similar technique was used by Merilees [17] for the south and north pole singularities of spherical coordinates but appears not to have been applied more generally. Here we show that the technique leads to excellent results for a number of model problems. The main application we consider is the compressible unsteady Euler and Navier–Stokes equations in cylindrical coordinates (Section 3). For comparison with other methods, we also treat the solution of Bessel’s equation in Section 4. Several

other problems [20] have been treated in an analogous way, but are not repeated here for brevity.

## 2. APPROACH

The present treatment of the  $1/r^n$  singularities in the radial direction can be summarized as follows:

- (i) A new radial coordinate is defined over both positive and negative radius

$$\tilde{r}(r, \phi) = \begin{cases} r & \text{if } 0 \leq \phi < \pi \\ -r & \text{if } \pi \leq \phi < 2\pi \end{cases} \quad (1)$$

as depicted in Fig. 1. This transformation has been already used in [7] to solve the Bessel's equation, but with a grid point at the pole and using the exact pole equation.

(ii) Differentiation is performed with respect to the new coordinate,  $\tilde{r}$ , but on a set of nodes which avoids the singularity. For FD schemes (on a uniform mesh), for example, we have

$$r_n = \frac{(2n+1)\Delta r}{2}; \quad n = 0, 1, 2, \dots \quad (2)$$

For PS schemes Chebyshev nodes (CN) with even number of points over  $-1 \leq \tilde{r} \leq 1$ ,

$$r_k = -\cos(\pi k/2N_r + 1), \quad k = 0, 1, \dots, 2N_r + 1 \quad (3)$$

will be suitable. These should be compared with, for example, the Chebyshev-Lobatto nodes (CLN) which are defined on  $0 \leq r \leq 1$  as

$$r_k = \frac{1 - \cos(k\pi/N_r)}{2}, \quad k = 0, 1, \dots, N_r \quad (4)$$

which give clustering around both  $r = 0$  and 1 and have been recommended for PS solutions of problems with pole singularities by Huang and Sloan [12].

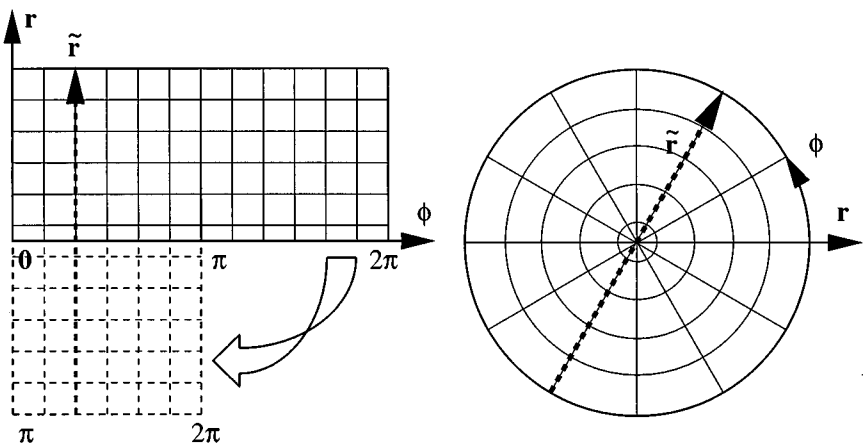


FIG. 1. Computational and physical domains.

(iii) Scalar and vector quantities must be transformed appropriately between the  $r$  to the  $\tilde{r}$  coordinates. The following simple *transformation rule* holds: when  $0 \leq \phi < \pi$  all quantities are the same in both coordinate systems. For  $\pi \leq \phi < 2\pi$  we multiply any polar components of a vector quantity, radial derivative, and any  $r$  by  $-1$ . For example, the convective term  $\partial(v_r v_\phi)/\partial r$  has exactly the same form and sign in both coordinates for  $0 \leq \phi < \pi$  while it has opposite sign (because of multiplication by three negative signs) for  $\pi \leq \phi < 2\pi$ .

Note that this transformation is only used to calculate the radial derivatives. For the azimuthal derivatives the traditional definition of cylindrical coordinate is used. Thus the new singularity which is generated in the azimuthal direction by redefining the radial coordinate is avoided. Furthermore, in the axisymmetric case one need not carry the computations over  $[-R, R]$ , but instead symmetry conditions can be used to close FD schemes at the point adjacent to the pole and parity properties may be used in PS schemes to reduce the number of equations by half. However, we would like to emphasize that the general approach *does not* depend on any parity property of the equations and can be used to find non-axisymmetric solutions. An example is provided in Section 3.

Here we show that the rule of transformation (iii), applied to an arbitrary regular function  $f$ , is consistent with the constraints on the behavior of its Fourier series coefficients near the pole. Therefore the transformation (iii) has no effect on the regularity of the function in the new coordinate. We take the Fourier series representation of an arbitrary function  $f(r, \phi)$ ,

$$f(r, \phi) = \sum_{m=-\infty}^{\infty} a_m(r) e^{im\phi}. \quad (5)$$

Now, if  $f$  is a regular scalar quantity, we must require that  $a_m(r) = r^{|m|} b_m(r^2)$  as  $r \rightarrow 0$ , where  $b_m(r^2)$  is a regular function of  $r^2$  [14]. In the  $(\tilde{r}, \tilde{\phi})$  coordinates the same representation is valid for  $0 \leq \phi < \pi$ . If  $\pi \leq \phi < 2\pi$  we substitute  $\phi = \tilde{\phi} + \pi$  and  $r = -\tilde{r}$ . Hence

$$f(r, \phi) = \sum_{m=-\infty}^{\infty} a_m(-\tilde{r}) e^{im(\tilde{\phi}+\pi)} = \sum_{m=-\infty}^{\infty} a_m(-\tilde{r}) (-1)^m e^{im\tilde{\phi}}. \quad (6)$$

But as  $r \rightarrow 0$ , we have  $a_m(-\tilde{r}) (-1)^m = a_m(\tilde{r})$  (see [14]), and thus the regularity of the function  $f$  is preserved in the new coordinate  $(\tilde{r}, \tilde{\phi})$ . The rule of transformation (iii) can be justified by applying the preceding analysis to functions of the form  $r^n f(r, \phi)$ , radial derivatives of  $f$ , and vector quantities.

In spherical coordinates  $(r, \phi, \theta)$  the pole singularities are caused by two factors:  $r \rightarrow 0$  and  $\sin(\phi) \rightarrow 0$ . The singularity of radial derivatives at  $r = 0$  can be treated as described above for cylindrical coordinates, i.e., by extending  $r$  to negative values and shifting the grid points in the radial direction by  $\Delta r/2$  so that there is no grid point at  $r = 0$ . The singularities at  $\phi = 0$  and  $\pi$  can be handled using a similar strategy (see Merilees [17] and Mohseni [20]).

The maximum allowable timestep for convective problems is usually controlled by the Courant–Friedrichs–Lewy (CFL) number. The effect of grid distributions on the CFL number has been the subject of previous research [3, 1]. Here we compare the CFL requirements for the present and conventional grid distributions.

A conservative estimate for the CFL number will depend on the minimum mesh spacing in any of the three coordinate directions. To simplify the argument, in the rest of this section we assume that the CFL criteria are the same in all directions.

For axisymmetric problems, the conventional grid defined by  $r_n = n\Delta r$ ;  $n = 0, 1, 2, \dots$ , gives a CFL constraint which is dependent on  $\Delta r$ . Despite the grid point at  $\Delta r/2$  in the modified grid (Eq. (2)) numerical experiments confirm that the CFL number continues to scale with  $\Delta r$ . For *non-axisymmetric* problems, the situation is different. For  $N_\phi$  Fourier or FD modes in the azimuthal direction, the minimum length of the mesh in the  $\phi$ -direction is now  $\pi \Delta r/N_\phi$ , half of the value for a conventional grid with the first node at  $\Delta r$ . Thus with no further modification, the maximum time step in the present approach is a factor of two smaller than other approaches. In either case, the CFL constraint is *very restrictive* in non-axisymmetric cylindrical coordinates, the minimum time step being proportional to the product of the grid spacing in  $r$  and  $\phi$ .

In both cases it is possible to alleviate this constraint by explicitly filtering the results in the  $\phi$  direction, as has been suggested by many investigators (e.g., [3] and references therein). Since the solution is periodic in the  $\phi$  direction it is possible to employ a sharp spectral filter at a particular cutoff wavenumber. For grids defined by  $r_n = n\Delta r$ ;  $n = 0, 1, 2, \dots$ , the effective mesh spacing in the  $\phi$  direction becomes  $\Delta x_\phi = 2\pi \Delta r/N_{f\phi}$  along the circle at  $r = \Delta r$ , where  $N_{f\phi}$  is the number of nodes retained. Thus if 7 or fewer nodes are retained the CFL constraint will be dictated by  $\Delta r$ . The maximal number of nodes of  $N_{f\phi} \approx 2\pi n$  that should be retained at different radial locations  $r_n$  follows in an analogous way. For the present grid, the first node is placed at  $\Delta r/2$ ; then we need merely retain fewer Fourier modes (at most  $N_{f\phi} \approx \pi n$ ) at each  $r_n$ , so that the CFL constraint depends on  $\Delta r$  alone (see [20] for numerical validation).

In PS methods, the clustering of node points near the boundaries also has an impact on the maximum CFL number. Since the pole is traditionally considered as a boundary point, the same clustering occurs at the poles (e.g., [12]). Fornberg [7] noticed that it is possible to alleviate the quadratic clustering of nodes near the origin, by defining the radial coordinate as in Eq. (1). We observe the same property in our grid distribution, except that our grid points are shifted so that no grid point is located at the pole. Therefore, one can choose the grid distribution in the  $\tilde{r}$  coordinate to dramatically increase the maximum timestep required for stability around the centerline for PS methods compared to other grid distributions. In fact, using the distributions given above, it can easily be shown that the distance from the centerline to the first node away from the centerline is  $N_r/\pi$  times greater for the CN distribution than for the CLN distribution, in the limit of large  $N_r$ . Thus the maximum timestep increases also by this factor.

Finally, we would like to point out that the present approach should not be confused with the idea of staggered grids (e.g., [6]). Here, we use the co-located discretization where the nodes are chosen to avoid singularities. Staggered grids require further modifications as discussed in [20].

### 3. COMPRESSIBLE NAVIER–STOKES EQUATIONS

We consider solution of the Navier–Stokes and Euler equations in cylindrical coordinates. One approach which has been used in the past is to superpose a Cartesian coordinate system at the singularity as was done, for example, in recent compressible jet calculations by Mitchell *et al.* [18, 19] and Freund *et al.* [8]. A different approach was used by Griffin *et al.* [11], where l’Hopital’s rule was used to the singular terms in the NS equations to derive a new set of equations valid at the centerline. These equations are then solved by one-sided difference schemes at the centerline. They observed a significant loss of accuracy

when the biased difference scheme used at the centerline was less accurate than the interior scheme. Various other schemes for the Navier–Stokes equations in cylindrical coordinates have been given in the literature [1, 15, 21, 22, 25].

Aside from the centerline treatment, the details of the numerical scheme used in this work are similar to the approach of Freund *et al.* [8]. At the outer radial boundary non-reflecting boundary conditions are implemented [9]. In the radial direction we use a sixth order accurate compact Padé scheme [13] and in the azimuthal direction a Fourier spectral method is used. For the purposes of this paper, only flows which are uniform in the axial direction are considered. Fourth order Runge–Kutta time advancement is used to advance the solution to the next timestep. This combination of high-order-accurate compact finite difference schemes and explicit Runge–Kutta time advancements has now been used in many codes developed for solving problems in compressible turbulence and aeroacoustics (e.g., [5, 8, 18, 19]).

For the centerline treatment, we implement two approaches: the first (CL1) uses the coordinate transformation and grid distribution discussed in the last section; the other (CL2) solves the equations in Cartesian coordinates at the centerline [8, 19, 18].

As an example, consider the propagation of a Gaussian acoustic pulse with unit variance located, initially, off-centered at  $(r = 1, \phi = 0)$  in cylindrical coordinates. The specific head ratio is 1.4. The outer radial non-reflecting boundary is placed at  $r = 8$ . The grid is 81 by 64 nodes in the radial and azimuthal directions, respectively. The acoustic pulse initially has the form of a small amplitude pressure and density disturbance superposed on their (constant) ambient values. In the present example, we take the magnitude of the acoustic pulse to be very small ( $10^{-6}$ ) such that nonlinear effects are minimal and an exact solution to the linearized version of this problem can be found [23] and compared to the numerical solution. In what follows, we give the density of the acoustic wave (less the ambient density) relative to the ambient density. Lengths are normalized by the variance (width) of the initial Gaussian pulse, and time is normalized using this length and the ambient sound speed. The timestep for these calculations is  $\Delta t = 0.003125$ .

In addition to a greater ease of implementation, we find that in viscous computations, method CL1 is stable with a much smaller viscosity (higher Re) than CL2. Long time instability of the inviscid method is characteristic of non-dissipative (centered) finite difference schemes in general and is not directly a consequence of the coordinate singularity. The instability is believed to result from aliasing of energy onto the highest wavenumbers supported by the grid (sawtooth waves) and repeated reflections (and, indeed, amplification) of these waves by the non-periodic boundaries. In Fig. 2 the numerical solution of inviscid equations for method CL1 is shown for times 2 and 4. The absolute errors are plotted for both CL1 and CL2 at time  $t = 2$  in Fig. 3. For CL2, poorly resolved sawtooth waves can be seen. It is clear that they are produced by the centerline treatment since the pulse is initially located off-center at  $r = 1$ . These short wavelength disturbances are continuously produced at the centerline. They are similar to the sawtooth waves studied by Trefethen [24], Vichnevetsky [26], and Colonius [4], where it has been shown that they can propagate at physically inappropriate (large and with incorrect sign) group velocities and that they are converted to smooth (well-resolved) waves upon interaction with boundary conditions (in this case at both  $r = 0$  and  $r = R$ ). By contrast, such spurious waves are not evident for treatment CL1, and the error (Fig. 3a) is centered at the center of the acoustic pulse and is almost 2 orders of magnitude smaller than CL2. This error is apparently controlled only by the finite resolution.

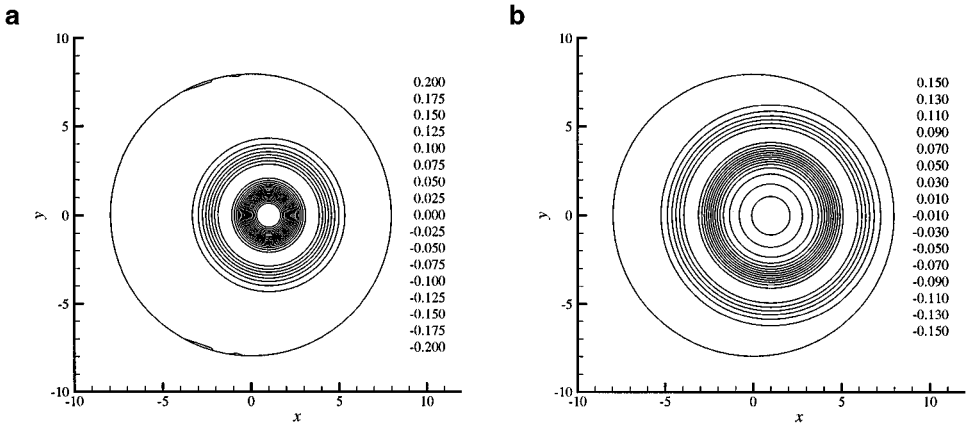


**FIG. 2.** Numerical solution (density perturbation relative to initial amplitude) for method CL1 at (a)  $t = 2$ , (b)  $t = 4$ .

#### 4. BESSEL'S EQUATION

To compare the method described above to previous treatments, we consider PS and FD solutions of Bessel's equation in cylindrical and spherical coordinates:

$$\frac{1}{r^a} \frac{d}{dr} \left( r^a \frac{dy}{dr} \right) - \frac{n(n+a-1)}{r^2} y = -\lambda y, \quad 0 \leq r \leq 1, \quad (7)$$

where  $n \geq 0$ , and  $a = 1, 2$  for Bessel's and spherical Bessel's equations, respectively. The boundary condition for both equations is given by  $y(1) = 0$ . The eigenvalues for the Bessel's equation are given analytically by  $\lambda_{np} = r_{np}^2$ , where  $r_{np}$  are the zeros of the Bessel's functions  $J: J_n(r_{np}) = 0, p = 1, 2, \dots$ . The solution to the equation is the spherical Bessel's equation  $j_n(r'_{np})$ , where  $r'_{np}$  are the zeros of  $j_n(r'_{np}), p = 1, 2, \dots$  and the eigenvalues are  $\lambda_{np} = r_{np}^2$ .

For Bessel's equation, Gottlieb and Orszag [10] improved the convergence of their Chebyshev tau method by using the pole condition  $y'(0) = 0$ . Huang and Sloan [12] showed that this pole condition does not give spectral accuracy for  $n = 1$ . They derived an improved

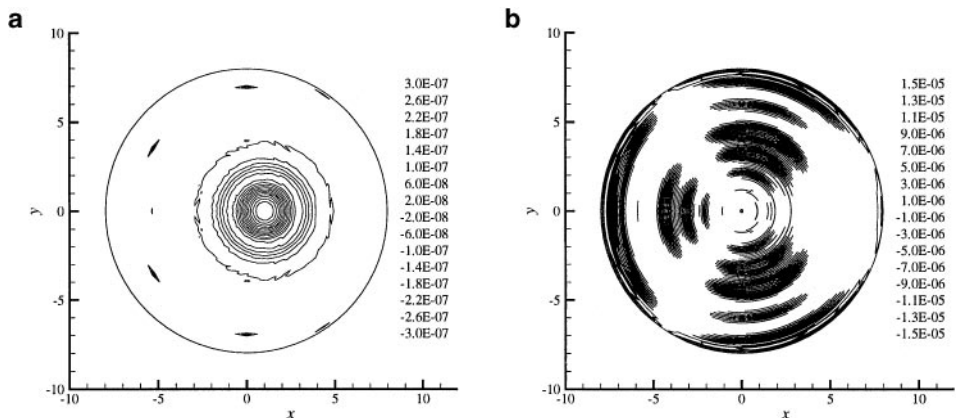


**FIG. 3.** Absolute error in solution at  $t = 2$  relative to the initial amplitude of the pulse for (a) CL1, (b) CL2.

pole condition for  $n = 1$  to preserve the spectral accuracy. Fornberg [7] used these pole equations but he changed the definition of the cylindrical coordinate (Eq. (1)) to allow the radial grid to run through the pole. In addition to more accuracy, he notes the possible advantage of not having a clustering of the nodes near  $r = 0$ . Note that unlike the present approach a node, and therefore a pole equation, is used at the singularity,  $r = 0$ . Recently, Matsushima and Marcus [16] found a new set of basis functions defined by a singular Sturm–Liouville equation so that the pole condition is maintained. They applied their method successfully to Bessel’s equation and the vorticity transport equation on a unit disk.

Here the present method is employed to solve Bessel’s equation with a PS method based on Lagrange’s interpolation formula [12] but without any pole conditions. We use the parity property of Bessel’s equation to reduce the calculation to only the positive half of the Chebyshev node distribution considered in Section 2:

$$r_k = \cos\left(\frac{\pi(k - N_r)}{2N_r + 1}\right), \quad k = 0, 1, \dots, N_r. \quad (8)$$

In Fig. 4 the convergence of the numerical solution to the exact eigenvalue is shown. The relative errors for the first eigenvalue,  $\lambda_{n1}$ , for  $n = 7$  and 49 are plotted for various PS schemes and a second order FD method with the present treatment of the singularity.

All of the solutions are very accurate, and for large  $N$  it becomes difficult to compare the relative accuracy of the schemes, since the error becomes dominated by roundoff even with double precision arithmetic. To overcome this problem and make reliable comparisons between methods, we recomputed the results with sufficient precision arithmetic using the *Mathematica* [27] program when necessary.

Apparently the new pole treatment gives spectral convergence and is more accurate for all  $N$  than that of Refs. [12, 16]. Matsushima and Marcus [16] pointed out that the spectral convergence of the Chebyshev expansion of Gottlieb and Orszag [10] deteriorates significantly as  $n$  becomes large. This effect was attributed to the shifting of the oscillatory part of the Bessel function moving toward the outer boundary as  $n$  increases. It is clear from the figure that our PS approach is not suffering from the oscillatory behavior of the solution near the boundary and gives better convergence. Finally, similar results for  $n = 1$  presented by Fornberg [7] overlap with our results for  $n = 1$ . However, his results were obtained using

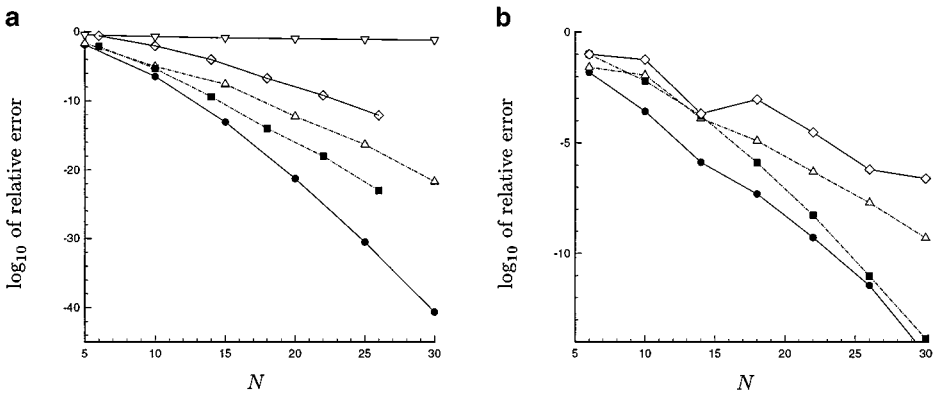


**FIG. 4.** First eigenvalues of the Bessel equation for (a)  $n = 7$ , (b)  $n = 49$ .  $\Delta$ , Huang and Sloan [12];  $\nabla$ , second order FD;  $\bullet$ , present approach;  $\diamond$ , Gottlieb and Orszag [10];  $\blacksquare$ , Matsushima and Marcus [16].

an exact pole equation which is not available for more complex equations, such as those considered in the previous section.

Finally the smallest eigenvalue of the spherical Bessel equation was also calculated numerically, and with the identical conclusions (see [20] for detail).

### ACKNOWLEDGMENTS

The authors thank Professor B. Fornberg for his helpful discussions and for bringing Ref. [17] to our attention. This research was supported by NSF under Grant CTS-9501349.

### REFERENCES

1. K. Akselvoll and P. Moin, An efficient method for temporal integration of the navier–stokes equations in confined axisymmetric geometries, *J. Comput. Phys.* **125**(2), 454 (1996).
2. K. Akselvoll and P. Moin, An efficient method for temporal integration of the navier–stokes equations in confined axisymmetric geometries, *J. Comput. Phys.* **125**(2), 454 (1996).
3. C. Canuto, M. Y. Hussaini, A. Quarteroni, and T. A. Zang, *Spectral Methods in Fluid Dynamics* (Springer-Verlag, New York/Berlin, 1987).
4. T. Colonius, Numerically nonreflecting boundary and interface conditions, for compressible flow and aeroacoustic computations, *AIAA J.* **35**(7), 1126 (1997).
5. T. Colonius, S. K. Lele, and P. Moin, Sound generation in a mixing layer, *J. Fluid Mech.* **330**, 375 (1997).
6. J. H. Ferziger and M. Peric, *Computational Methods for Fluid Dynamics* (Springer-Verlag, New York/Berlin, 1996).
7. B. Fornberg, *A Practical Guide to Pseudo-spectral Methods* (Cambridge Univ. Press, Cambridge, UK, 1996).
8. J. B. Freund, S. K. Lele, and P. Moin, *Direct Simulation of a Supersonic Round Turbulent Shear Layer*, AIAA Paper 97-0760, 1997.
9. M. Giles, Non-reflecting boundary conditions for Euler equations, *AIAA J.* **28**(12), 2050 (1990).
10. D. Gottlieb and S. A. Orszag, *Numerical Analysis of Spectral Methods: Theory and Applications* (Soc. for Industr. & Appl. Math., Philadelphia, 1977).
11. M. D. Griffin, E. Jones, and J. D. Anderson, A computational fluid dynamic technique valid at the centerline for non-axisymmetric problems in cylindrical coordinates, *J. Comput. Phys.* **30**, 352 (1979).
12. W. Huang and D. M. Sloan, Pole condition for singular problems: The pseudo-spectral approximation, *J. Comput. Phys.* **107**, 254 (1993).
13. S. K. Lele, Compact finite difference schemes with spectral-like resolution, *J. Comput. Phys.* **103**(1), 16 (1992).
14. H. R. Lewis and P. M. Bellan, Physical constraints on the coefficients of Fourier expansions in cylindrical coordinates, *J. Math. Phys.* **31**(1), 2592 (1990).
15. R. R. Mankbadi, M. E. Hayer, and L. A. Povinelli, Structure of supersonic jet flow and its radiated sound, *AIAA J.* **32**(5), 897 (1994).
16. T. Matsushima and P. S. Marcus, A spectral method for polar coordinates, *J. Comput. Phys.* **120**, 365 (1995).
17. P. E. Merilees, The pseudospectral approximation applied to the shallow water equations on a sphere, *Atmosphere* **11**(1), 13 (1973).
18. B. E. Mitchell, S. K. Lele, and P. Moin, *Direct Computation of the Sound Generated by Subsonic and Axisymmetric Jets*, Report No. TF-66, Department of Mechanical Engineering, Stanford University, 1995.
19. B. E. Mitchell, S. K. Lele, and P. Moin, Direct computation of the sound generated by an axisymmetric jet, *AIAA J.* **35**(10), 1574 (1997).
20. K. Mohseni, Investigations on coherent structures: A. Universality in vortex formation; B. Evaluation of noise generation mechanisms in fully expanded supersonic jets, Ph.D. Thesis, California Institute of Technology, Pasadena, CA, January 2000.

21. P. J. Morris, L. N. Long, A. Bangalore, and Q. Wang, A parallel three-dimensional computational aeroacoustic method using nonlinear disturbance equations, *J. Comput. Phys.* **133**, 56 (1997).
22. S. H. Shih, R. Hixon, and R. R. Mankbadi, *Three Dimensional Structure in a Supersonic Jet: Behavior near Centerline*, AIAA Paper 95-0681, 1995.
23. C. K. W. Tam and J. C. Webb, Dispersion relation preserving finite difference schemes for computational acoustics, *J. Comput. Phys.* **107**, 262 (1993).
24. L. N. Trefethen, Group velocity in finite difference schemes, *SIAM Rev.* **124**(2), 113 (1982).
25. R. Verzicco and P. Orlandi, A finite-difference scheme for three-dimensional incompressible flows in cylindrical coordinates, *J. Comput. Phys.* **123**, 402 (1996).
26. R. Vichnevetsky and J. B. Bowles, *Fourier Analysis of Numerical Approximations of Hyperbolic Equations* (Soc. for Industr. & Appl. Math., Philadelphia, 1982).
27. S. Wolfram, *Mathematica*, 2.2 ed. (Wolfram Research, Inc., 1994).